Recrystallization in an Mg-Nd alloy processed by high-pressure torsion: a calorimetric analysis

Yousf Islem Bourezg[1,2], Hiba Azzeddine[3*], Khadidja Abib[1], Yi Huang[4, 5], Djamel Bradai[1], Terence G. Langdon[4]

[1] Faculty of Physics, University of Sciences and Technology Houari Boumediene, Algiers, Algeria

[2]Department of Physics, Ziane Achour University of Djelfa, BP 3117 Djelfa, Algeria

[3] Faculty of Technology, University of Mohamed Boudiaf, M'sila, Algeria

[4]Materials Research Group, Department of Mechanical Engineering, University of Southampton, Southampton SO17 1BJ, UK

[5]Department of Design and Engineering, Faculty of Science and Technology, Bournemouth University, Poole, Dorset BH12 5BB, UK

Abstract

Differential scanning calorimetry (DSC) was used to evaluate the recrystallization temperature and activation energy for an Mg-1.43Nd (wt.%) alloy after severe plastic deformation by high-pressure torsion (HPT) at room temperature up to 10 turns. The recrystallization kinetics were determined from DSC analysis. The results show that the recrystallization temperature increases with increasing heating rate and decreases with increasing numbers of HPT turns. Severe plastic deformation by HPT significantly reduces the recrystallization temperature. The estimated activation energy for recrystallization was in the range of ~ 84-89 kJ mol^{-1}.

Keywords: Activation energy; Differential Scanning Calorimetry; High-pressure torsion; Mg-Nd alloy; Recrystallization.

[*]Corresponding author: Dr. Hiba AZZEDDINE, email: azehibou@yahoo.fr

1. Introduction

Magnesium and its alloys have increasingly attracted scientific investigations because of potential applications in the aerospace and transportation industries due to their high specific strength and attractive environmental characteristics [1, 2]. Nevertheless, magnesium alloys suffer from poor formability at low temperatures because of their hexagonal crystallography and the consequent lack of sufficient numbers of independent slip systems. Several strategies have been proposed to overcome this deficiency. Recent work [3–7] showed that a modification of the chemical composition of Mg alloys with special emphasis on the addition of rare earth (RE) elements may potentially improve the plastic formability. Thus, RE elements may change the deformation mechanisms during plastic deformation by introducing solute drag and thereby changing the relative boundary mobility [8] and/or by enhancing the activation of hard systems such as <*c* + *a*> pyramidal slip [9–11]. In addition, Mg-RE precipitates tend to inhibit grain growth during hot working or annealing and ensure good thermal stability of the refined microstructures [12].

Severe plastic deformation (SPD) techniques, such as equal-channel angular pressing (ECAP) [13] and high-pressure torsion (HPT) [14], were found to significantly enhance the room temperature ductility of a range of magnesium alloys [15–18] and in practice SPD techniques have the potential of producing ultra-fine grained (UFG) materials and alloys characterized by excellent mechanical and physical properties such as high yield strength and superplasticity. These enhanced properties are due to a combination of the UFG microstructure and the introduction of considerable amounts of defects. Nevertheless, the processing of Mg alloys by ECAP is generally restricted to relatively high temperatures [19, 20] in order to avoid billet cracking and the segmentation along the gauge section that is often observed after ECAP at room temperature. By contrast, processing by HPT prevents the development of segmentation and cracking due to the large imposed hydrostatic pressure [21] and this provides an opportunity for producing a UFG structure, even in pure magnesium, by processing using HPT at room temperature (RT) [22]. Processing by HPT also has an advantage over ECAP because it leads to both a more refined microstructure [23, 24] and a higher fraction of grain boundaries having high angles of misorientation [25].

Post-deformation annealing (PDA) treatments of UFG materials are often used in order to attain a reasonably stable state by recovery and recrystallization [26, 27] and therefore it is important to investigate the thermal stability of UFG materials. The recrystallization of Mg-based alloys after conventional deformation processing has been widely investigated [28–32]. However, there are only limited reports of PDA after SPD processing at elevated temperatures [33] and the role of PDA after processing of Mg alloys at RT appears to be restricted to samples that were heavily cold worked but not subjected to new SPD processing [34]. Accordingly, the present investigation was initiated in order to evaluate, using differential scanning calorimetry (DSC), the recrystallization temperature and the kinetics as well as the activation energy in a Mg-1.43Nd (wt.%) alloy after processing by HPT at RT for up to 10 turns.

2. Methods

The material used in this investigation was Mg-1.43Nd (wt.%) with the alloy provided in an as-cast state by the Institut für Metallkunde und Metallphysik (IMM, RWTH), Aachen, Germany.

Discs with thicknesses of 1.5 mm and diameters of 10 mm were partially solutioned in sealed glass tubes by holding at 535 °C for 5 h and then carefully polishing to final thicknesses of ~0.85 mm. The HPT processing was conducted at RT

using a rotational speed of 1 rpm and quasi-constrained conditions [35, 36] for 1/2, 1, 5 and 10 turns using an imposed pressure of 6.0 GPa.

Small samples of 18−20 mg and with a diameter of 5 mm were cut near the centers of the HPT discs in order to perform a DSC analysis using a 2920 MDSC calorimeter under constant heating rates of 10, 20, 30 and 40 °C/min in a nitrogen atmosphere. The DSC scanning temperature ranged from 80 to 500 °C

3. Results

Fig. 1 presents the DSC thermograms of the Mg-1.43Nd alloy subjected to 1/2, 1, 5 and 10 HPT turns obtained by continuous heating with a 20 °C/min rate. Other scans corresponding to 5, 10 and 30 °C/min are not included in this report since they exhibit almost identical trends. All of the thermograms show five exothermic peaks which are labeled in Fig. 1 as Rex, β"', β_1, β and β_e and two endothermic peaks labeled D_1 and D_2. The first exothermic peak around 180 °C corresponds to the recrystallization event. Observations of this type of precipitation sequence are generally in good agreement with those described earlier [37, 38]. The results of an investigation of the sequence and a quantitative analysis of the precipitation processes in the Mg-1.43Nd alloy after HPT processing were published in an earlier report [39].

Fig. 2 and 3 show the DSC scans of the recrystallization peaks and the corresponding values of the temperature peaks of recrystallization as a function of the numbers of HPT turns for heating rates of 5, 10, 20 and 30 °C/min, respectively. It is clear from these data that the peak temperature of the recrystallization phenomena increases with increasing heating rate and decreases with increasing numbers of HPT turn. The present results show that the recrystallization temperature is in the range of 138–175 °C. The presence of an exothermic peak below 200 °C belonging to the recrystallization was already reported in Mg-1.44Ce (wt.%) [40] and Mg-0.41Dy (wt.%) alloys [41] after HPT processing at RT up to 10 and 5 turns, respectively.

In order to evaluate the activation energy for recrystallization, the Boswell-Kissinger method was used based on the DSC measurements according to the following equation [42]:

$$\ln \frac{V}{T_p} = C - \frac{E}{RT_p} \qquad (1)$$

where V is the heating rate, $E$is the activation energy, $T_p$is the maximum temperature of the peak, R is the universal gas constant and C is a constant.

In order to make use of equation (1), Fig.4 shows the evolution of $\ln(V/T_p)$ as a function of $(1000/T_p\ K^{-1})$ for the recrystallization peaks measured by DSC using the four heating rates of 5, 10, 20 and 30 °C/min after processing the alloy by HPT for up to 10 turns. It is evident that this Boswell-Kissinger plot shows straight lines and the activation energy can be determined directly from the slope of the plot. Thus, the values deduced for the activation energy for recrystallization are given in Fig.5 as functions of the numbers of HPT turns. It is readily evident that the activation energy decreases significantly between 1/2 and 1 HPT turns but thereafter it only gradually decreases between 1 and 10 turns. With a maximum error of ΔT_p ~2 °K and ΔV ~0.5 °K/min, the relative error of the activation energy deduced from (eq.1) amounts roughly to $\Delta E/E < 10$ %.

The kinetics of recrystallization can be determined during the DSC analysis using the following relationship [43]:

$$F_v = \frac{A_T}{A} \qquad (2)$$

where *Fv* is the recrystallized volume fraction, *A* is the total area of the exothermic peak and A_T is the area between the onset peak and the chosen temperature T, respectively.

Fig. 6 (a-d) shows the recrystallized volume fraction of the Mg-1.43Nd alloy after HPT processing to 1/2, 1, 5 and 10 turns calculated from the DSC analysis at the different heating rates of 5 (a), 10 (b), 20 (c) and 30 °C/min (d). Thus, sigmoidal-shaped curves are obtained and there is a clear shift in the recrystallized fraction to lower temperatures with an increase in the imposed strain introduced by the HPT processing. There is also a clear shift of the curves to higher temperature with increasing heating rate.

4. Discussion

Based on these experimental results, it is possible to rationalize the overall decomposition sequence in the Mg-1.43Nd alloy. It is clear that after the HPT processing of this alloy the recrystallization phenomenon is concomitant with a complex sequence of precipitation reactions. Nevertheless, for all of the samples the DSC analysis exhibits a five-stage precipitation sequence and this is generally in agreement with the sequences proposed in some earlier reports [37, 38].

Based on an extensive review of the recrystallization of duplex alloys, it appears that the present observations obey Regime III following the scheme proposed in this earlier review [44]. During regime III, the recrystallization becomes complete before the occurrence of significant precipitation and thus it appears to be influenced only by solute segregation so that precipitation subsequently occurs in the recrystallized material. The use of HPT processing on the Mg-1.43Nd alloy at RT does not seem to significantly affect this sequence. However as shown in Fig. 3, the recrystallization temperature was lowered considerably (138–175°C) in the current investigation relative to conventional plastic deformation. It was reported that among Mg-RE alloys the Mg-Nd exhibits the highest onset temperature of recrystallization [45]. As an example, for a cold-rolled Mg-2.65Nd (wt. %) alloy the recrystallization temperature was about 300 °C and it is believed that the recrystallization temperature is strongly affected by simultaneous precipitation during the recrystallization process [30, 31, 45]. By contrast, the present results show that the severe plastic deformation introduced by HPT considerably influences the recrystallization temperature in the absence of any simultaneous precipitation. It was reported in the Mg-1.44Ce (wt%) alloy after HPT processing up to 10 turns that the recrystallization peak temperature was considerably reduced within the range of ~135–177.1 °C [40]. It was found also in the Mg-0.41Dy (wt.%) alloy processed by HPT up to 5 turns that the recrystallization process was completed within the range of ~120–200 °C [41] and the recrystallization temperature increased with increasing heating rate.

The activation energies for recrystallization derived from the present investigation ranges from ~84 to ~89 kJ mol^{-1} for 10 and 1/2 turn of HPT, respectively. It is noted that the activation energy for dislocation release is not dependent upon the strain value, at least for shear strains $\gamma \leq 15$ [46], but HPT processing is known to result in a very strong equivalent strain of more than 200 after 10 turns. It is apparent that the activation energy is lower than the value for self-diffusion in magnesium (~135 kJ mol^{-1}) and slightly lower than the value for boundary self-diffusion (~92 kJ mol^{-1}) [47]. Close values of ~72 to ~87 kJ mol^{-1} were reported in Mg-Ce alloy processed by HPT at RT [40]. The activation energies of the recrystallization were around ~86 kJ mol^{-1} in a heavily cold-drawn and annealed AZ31 alloy [34]. Furthermore, there is a report of a similar value of ~69–88 kJ mol^{-1} [48] in twin-roll cast (TRC) AZ31 magnesium alloy and

the activation energy for recrystallization in an Mg-0.42Nd (wt.%) alloy was ~120 kJ mol^{-1} [49]. Thus, the lower values of the activation energy for recrystallization obtained after SPD processing is probably associated with the high density of nucleation sites compared with conventional deformation, including the presence of high-angle grain boundaries and a high concentration of both single/double vacancies and/or vacancy agglomerates [46, 50]. Moreover, there is a considerable increase in the density of vacancies during the SPD processing and this substantial increase may be partly due to the special conditions associated with the SPD processing. Both dynamic and static recovery and/or recrystallization processes were recently reported during and after SPD [51]. Furthermore, besides lowering the recrystallization temperature and activation energy, it is evident from Fig. 6 that there is a shift in the recrystallized volume fraction, *Fv*, to lower temperatures upon increasing the strain by HPT. Unfortunately, at present very little information is available on the nature of the static continuous recrystallization (SRX) kinetics and grain growth in Mg-based alloys in general and especially in Mg-RE alloys [28, 30].

It is now well established that dynamic recrystallization (DRX) is commonly observed during conventional hot deformation of magnesium and its alloys [52]. Specifically, DRX in magnesium alloys has been the focus of several studies [53–55]. A model was built for simulating static recrystallization processes that incorporates local effects such as the misorientations between elements and variations in the stored energy [56]. The experimental results obtained in plane strain compression of zinc samples were generally in good agreement with the simulated recrystallization kinetics [56] and both the experimental results and the predictions were consistent with a mechanism whereby nucleation occurs in highly-deformed domains and controls the recrystallization kinetics.

The values of the onset peak (T_0), the offset peak (T_{Max}), the recrystallization temperature (T_{Rex}) and the stored energy obtained from the DSC curves at heating rates of 5 °C.min^{-1} for the Mg-1.43Nd alloy after HPT processing up to 1/2, 1, 5 and 10 turns are documented in Table 1.The recrystallization temperature is conventionally defined as the temperature at which the material is 50 % recrystallized [57]. The stored energy, *E*, released during recrystallization in the DSC experiments corresponds to the area under the recrystallization peak in Fig. 2. There is an obvious shift of the recrystallization temperature to lower temperatures in Fig. 2 and 3 with increasing numbers of HPT turns. It is also apparent that the stored energy increases from 1/2 to 1 HPT turn and then decreases between 1 and 10 HPT turns. Such evolution of the stored energy versus strain is consistent with other observations where high purity copper and a ZK60 alloy were subjected to 4 and 8 passes of ECAP, respectively [58, 59].

Based on the data presented in Fig. 5 and Table 1, the Mg-1.43Nd alloy exhibits a higher activation energy for recrystallization and lower stored energy after the early stage of HPT at 1/2 turn. Therefore, the recrystallization process is less impeded upon increasing the strain level by the introduction of large amounts of defects and recrystallization sites. In Table 1, it is apparent also that there is an unusual evolution of the stored energy versus the strain level. Thus, there is an obvious shift of the recrystallization temperature to lower temperatures with increasing numbers of HPT turns. Typically, published data reveal a gradual increment of the stored energy up to a certain strain level, and thereafter the stored energy appears to level off to a reasonably saturated value [39, 60–62]. The stored energy introduced by SPD is known to increase the driving force for nucleation of new strain-free grains so that nucleation is then achieved at lower temperatures and therefore the activation energy

of recrystallization is reduced [63]. Nevertheless, in the material used in this investigation it appears that a mechanism for the formation of new grains through dynamic recrystallization, which thereby decreases the overall stored energy, is the key to attaining a full understanding of the observed behavior.

It is interesting to note that such behavior was already reported in a ZK60 alloy processed by ECAP for up to 4 passes at 250 °C [64]. It is reasonable to anticipate that HPT processing at room temperature may effectively cause dynamic recrystallization since it introduces far more defects than processing by ECAP even at warm temperatures and equivalent strains [65]. The proportion of high-angle grain boundaries (HAGBs) increases as recrystallization occurs and this latter is related to the formation and migration of HAGBs driven by the stored energy [64, 66]. In order to more fully confirm these suggestions, it will be necessary to conduct a systematic analysis of the microstructural evolution using an EBSD technique.

5. Conclusions

1. High pressure torsion (HPT) was applied to an Mg-1.43Nd alloy up to 10 turns at room temperature and the recrystallization temperatures and activation energies for recrystallization were estimated using differential scanning calorimetry.
2. The results show that the recrystallization phenomenon follows a complex sequence of precipitation reactions. The recrystallization temperature increases with increasing heating rate and decreases with increasing numbers of HPT turns. The activation energy for recrystallization is in the range from ~84 to 89 kJ mol^{-1} and decreases with increasing turns.
3. It is shown that processing by severe plastic deformation using HPT lowers the recrystallization temperature and leads to a decreasing stored energy with increasing turns.

Acknowledgements

One of the authors (YIB) wishes to heartily thank Prof. Jose Maria Cabrera from Polytecnia ETSEIB, Universidad Politécnica de Cataluña (UPC), for an invitation to UPC and for help during the scientific research and to the staff of the Biomaterials research group of UPC for their support in the DSC analysis. Two authors were supported by the European Research Council under ERC Grant Agreement No. 267464-SPDMETALS (YH and TGL).

References

[1] Agnew S R, Nie J F (2010) Preface to the viewpoint set on: The current state of magnesium alloy science and technology, Scr Mater 63:671–673. https://doi.org/10.1016/j.scriptamat.2010.06.029

[2] Suh B C, Shim M S, Shin K S, Kim N J (2014) Current issues in magnesium sheet alloys, Scr Mater 84–85: 1–6. https://doi.org/10.1016/j.scriptamat.2014.04.017

[3] Masoudpanah S M, Mahmudi R (2009) Effects of rare-earth elements and Ca additions on the microstructure and mechanical properties of AZ31 magnesium alloy processed by ECAP, Mater Sci Eng A 526: 22–30. https://doi.org/10.1016/j.msea.2009.08.027

[4] Wu B L, Zhao Y H, Du X H, Zhang Y D, Wagner F, Esling C (2010) Ductility enhancement of extruded magnesium via yttrium addition, Mater Sci Eng A 527:4334–4340. https://doi.org/10.1016/j.msea.2010.03.054

[5] Yan H, Chen R S, Han E H (2011) A comparative study of texture and ductility of Mg–1.2Zn–0.8Gd alloy fabricated by rolling and equal channel angular extrusion, Mater Character 62: 321–326. https://doi.org/10.1016/j.matchar.2011.01.005
[6] Zhu T, Sun J, Cui C, Wu R, Betsofen S, Leng Z, Zhang J, Zhang M (2014) Influence of Y and Nd on microstructure, texture and anisotropy of Mg–5Li–1Al alloy, Mater Sci Eng A 600:1–7. https://doi.org/10.1016/j.msea.2014.02.017
[7] Elfiad D, Bourezg Y I, Azzeddine H, Bradai D (2016) Investigation of texture, microstructure, and mechanical properties of a magnesium-lanthanum alloy after thermo-mechanical processing, Int J Mater Res 107: 315–323. https://doi.org/10.3139/146.111347
[8] Mackenzie L W F, Davis B, Humphreys F J, Lorimer G W (2007) The deformation, recrystallization and texture of three magnesium alloy extrusions, Mater Sci Tech 23: 1173–1180. https://doi.org/10.1179/174328407X226509
[9] Agnew S R, Yoo M H, Tomé C N (2001) Application of texture simulation to understanding mechanical behavior of Mg and solid solution alloys containing Li or Y, Acta Mater 49: 4277–4289. https://doi.org/10.1016/S1359-6454(01)00297-X
[10] Cottam R, Robson J, Lorimer G, Davis B (2008) Dynamic recrystallization of Mg and Mg–Y alloys: crystallographic texture development, Mater Sci Eng A 485: 375–382. https://doi.org/10.1016/j.msea.2007.08.016
[11] Stanford N (2010) Micro-alloying Mg with Y, Ce, Gd and La for texture modification–A comparative study, Mater Sci Eng A 527: 2669–2677. https://doi.org/10.1016/j.msea.2009.12.036
[12] Li X, Al-Samman T, Gottstein G (2011) Microstructure development and texture evolution of ME20 sheets processed by accumulative roll bonding, Mater Lett 65: 1907–1910. https://doi.org/10.1016/j.matlet.2011.03.104
[13] Valiev R Z, Langdon T G (2006) Principles of equal-channel angular pressing as a processing tool for grain refinement, Prog Mater Sci 51: 881–981. https://doi.org/10.1016/j.pmatsci.2006.02.003

[14] Zhilyaev A P, LangdonT G (2008) Using high-pressure torsion for metal processing: Fundamentals and applications, Prog Mater Sci 53: 893–979. https://doi.org/10.1016/j.pmatsci.2008.03.002
[15] Kim W J, An C W, Kim Y S, Hong S I (2002) Mechanical properties and microstructures of an AZ61 Mg Alloy produced by equal channel angular pressing, Scr Mater 47: 39–44. https://doi.org/10.1016/S1359-6462(02)00094-5
[16] Agnew S R, Horton J A, Lillo T M, Brown D W (2004) Enhanced ductility in strongly textured magnesium produced by equal channel angular processing, Scr Mater 50: 377–381. https://doi.org/10.1016/j.scriptamat.2003.10.006
[17] Edalati K, Yamamoto A, Horita Z, Ishihara T (2011) High-pressure torsion of pure magnesium: Evolution of mechanical properties, microstructures and hydrogen storage capacity with equivalent strain, Scr Mater 64: 880–883. https://doi.org/10.1016/j.scriptamat.2011.01.023
[18] Meng F, Rosalie J M, Singh A, Somekawa H, Tsuchiya K (2014) Ultrafine grain formation in Mg-Zn alloy by in situ precipitation during high-pressure torsion, Scr Mater 78–79:57–60. https://doi.org/10.1016/j.scriptamat.2014.01.036
[19] Kang F, Wang J T, Peng Y (2008) Deformation and fracture during equal channel angular pressing of AZ31 magnesium alloy, Mater Sci Eng A 487: 68–73. https://doi.org/10.1016/j.msea.2007.09.063

[20] Figueiredo R B, Langdon T G (2010) Grain refinement and mechanical behaviour of a magnesium alloy processed by ECAP, J Mater Sci 45: 4827–4836. https://doi.org/10.1007/s10853-010-4589-y
[21] Huang Y, Figueiredo R B, Baudin T, Helbert A L, Brisset F, Langdon T G (2013) Microstructure and texture evolution in a magnesium alloy during processing by high-pressure torsion, Mater Res 16: 577–585. http://dx.doi.org/10.1590/S1516-14392013005000025
[22] Figueiredo R B, Sabbaghianrad S, Giwa A, Greer J R, Langdon T G (2017) Evidence for exceptional low temperature ductility in polycrystalline magnesium processed by severe plastic deformation, Acta Mater 122: 322–331. https://doi.org/10.1016/j.actamat.2016.09.054
[23] Zhilyaev A P, Kim B K, Nurislamova G V, Baró M D, Szpunar J A, Langdon T G (2002) Orientation imaging microscopy of ultrafine-grained nickel, Scr Mater 46: 575–580. https://doi.org/10.1016/S1359-6462(02)00018-0
[24] Zhilyaev A P, Nurislamova G V, Kim B K, Baró M D, Szpunar J A, Langdon T G (2003)Experimental parameters influencing grain refinement and microstructural evolution during high-pressure torsion, Acta Mater 51: 753–765. https://doi.org/10.1016/S1359-6454(02)00466-4
[25] Wongsa-Ngam J, Kawasaki M, Langdon T G (2013) A comparison of microstructures and mechanical properties in a Cu-Zr alloy processed using different SPD techniques, J Mater Sci 48: 4653–4660. https://doi.org/10.1007/s10853-012-7072-0
[26] Andreau O, Gubicza J, Zhang N X, Huang Y, Jenei P, Langdon T G (2014) Effect of short-term annealing on the microstructure and flow properties of an Al-1% Mg alloy processed by high-pressure torsion, Mater Sci Eng A615: 231–239. https://doi.org/10.1016/j.msea.2014.07.018
[27] Maury N, Zhang N X, Huang Y, Zhilyaev A P, Langdon T G (2015) A critical examination of pure tantalum processed by high-pressure torsion, Mater Sci Eng A 638:174–182. https://doi.org/10.1016/j.msea.2015.04.053
[28] Abdessameud S, Bradai D (2009) Microstructure and texture evolution in hot rolled and annealed magnesium alloy TRC AZ31, Can Metall Q 48: 433–442. https://doi.org/10.1179/cmq.2009.48.4.433
[29] Yang X Y, Zhu Y K, Miura H, Sakai T (2010) Static recrystallization behavior of hot-deformed magnesium alloy AZ31 during isothermal annealing, Trans Non ferr Metals Soc China 20: 1269–1274. https://doi.org/10.1016/S1003-6326(09)60289-2
[30] Azzeddine H, Bradai D (2012) On the texture and grain growth in hot-deformed and annealed WE54 alloy, Int J Mater Res11: 1351–1360. https://doi.org/10.3139/146.110768
[31] Azzeddine H, Bradai D (2012) Texture and microstructure of WE54 alloy after hot rolling and annealing, Mater Sci Forum 702-703: 453–456. https://doi.org/10.4028/www.scientific.net/MSF.702-703.453
[32] Alili B, Azzeddine H, Abib K, Bradai D (2013) Texture evolution in AZ91 alloy, Trans Nonferr Metals Soc China 23: 2215–2221. https://doi.org/10.1016/S1003-6326(13)62720-X
[33] Stráska J, Janeček M, Čížek J, Stráský J, Hadzima B (2014) Microstructure stability of ultra-fine grained magnesium alloy AZ31 processed by extrusion and equal-channel angular pressing (EX–ECAP), Mater Character 94: 69–79. https://doi.org/10.1016/j.matchar.2014.05.013

[34] Chao H Y, Sun H F, Chen W Z, Wang E D.Static recrystallization kinetics of a heavily cold drawn AZ31 magnesium alloy under annealing treatment. Mater Character 2011; 62: 312–20. https://doi.org/10.1016/j.matchar.2011.01.007

[35] Figueiredo R B, Cetlin P R, Langdon T G. Using finite element modeling to examine the flow processes in quasi-constrained high-pressure torsion. Mater Sci Eng A 2011; 528: 8198–204. https://doi.org/10.1016/j.msea.2011.07.040

[36] Figueiredo R B, Pereira P H R, Aguilar M T P, Cetlin P R, Langdon T G. Using finite element modeling to examine the temperature distribution in quasi-constrained high-pressure torsion. Acta Mater 2012; 6: 3190–8. https://doi.org/10.1016/j.actamat.2012.02.027

[37] Nie J F. Precipitation and hardening in magnesium alloys. Metall Mater Trans A 2012; 43: 3891–939. https://doi.org/10.1007/s11661-012-1217-2

[38] Natarajan A R, Solomon E L S, Puchala B, Marquis E A, Van der Ven A. On the early stages of precipitation in dilute Mg–Nd alloys. Acta Mater 2016 108: 367–79. https://doi.org/10.1016/j.actamat.2016.01.055

[39] Bourezg Y I, Azzeddine H, Hennet L, Thiaudière D, Huang Y, Bradai D, Langdon T G . The sequence and kinetics of pre-precipitation in Mg-Nd alloys after HPT processing: A synchrotron and DSC study. J Alloys Compd 2017; 719: 236–41. https://doi.org/10.1016/j.jallcom.2017.05.166

[40] Bourezg Y I, Azzeddine H, Huang Y, Bradai D, Langdon TG. Investigation of recrystallization kinetics by DSC analysis of Mg-Ce alloy after severe plastic deformation. In: In Metal 2017: 26th International Conference on Metallurgy and Materials : May 24th-26th 2017, Hotel Voronez I, Brno, Czech Republic, EU. p. 1524–9.

[41] Hanna A, Azzeddine H, Lachhab R, Baudin T, Helbert A-L, Brisset F, Huang Y, Bradai D, Langdon T G (2019) Evaluating the textural and mechanical properties of an Mg-Dy alloy processed by high-pressure torsion, J Alloys Compd 778: 61–71. https://doi.org/10.1016/j.jallcom.2018.11.109

[42] Boswell P G (1980) On the calculation of activation-energies using a modified Kissinger method, J Therm Anal 18: 353–358. https://doi.org/10.1007/BF02055820

[43] Benchabane G, Boumerzoug Z, Thibon I, Gloriant T (2008) Recrystallization of pure copper investigated by calorimetry and microhardness, Mater Character 59: 1425–1428. https://doi.org/10.1016/j.matchar.2008.01.002

[44] Hornbogen E, Köster V (1978) Recrystallization of Metallic Materials, Stuttgart, Dr. Rieder Verlag.

[45] Rokhlin L L (2003) Magnesium alloys containing rare earth metals: structure and properties, Advances in Metallic Alloys. Taylor & Francis, London.

[46] Setman D, Schafler E, Korznikova E, Zehetbauer M J (2008) The presence and nature of vacancy type defects in nanometals detained by severe plastic deformation, Mater Sci Eng A 493:116–122. https://doi.org/10.1016/j.msea.2007.06.093

[47] Frost H J, Ashby M F (1982) Deformation Mechanism Maps. Pergamon, Oxford, U.K.

[48] Zhao H, Li P J, He L J (2011) Kinetics of recrystallization for twin-roll casting AZ31 magnesium alloy during homogenization, Intl J Miner Metall Mater18: 570–575. https://doi.org/10.1007/s12613-011-0479-9
[49] Rokhlin L L, Nikitina N I (1996) Investigation of recrystallization in an alloy of the Mg-Y-La-Zr system, Metal Sci Heat Treat 38: 171–173. https://doi.org/10.1007/BF01401515
[50] Hazra S S, Gazder A A, Pereloma E V (2009) Stored energy of a severely deformed interstitial free steel, Mater Sci Eng A 524: 158–167. https://doi.org/10.1016/j.msea.2009.06.033
[51] Zehetbauer M J, Steiner G, Schafler E, Korznikov A, Korznikova E (2006) Deformation induced vacancies with severe plastic deformation: Measurements and modeling, Mater Sci Forum 503-504: 57–64. https://doi.org/10.4028/www.scientific.net/MSF.503-504.57
[52] Cottam R, Robson J, Lorimer G, Davis B (2008) Dynamic recrystallization of Mg and Mg–Y alloys: Crystallographic texture development, Mater Sci Eng A 485: 375–382. https://doi.org/10.1016/j.msea.2007.08.016
[53] Galiyev A, Kaibyshev R, Gottstein G (2001) Correlation of plastic deformation and dynamic recrystallization in magnesium alloy ZK60, Acta Mater 49: 1199–1207. https://doi.org/10.1016/S1359-6454(01)00020-9
[54] Galiyev A, Kaibyshev R, Sakai T (2003) Continuous dynamic recrystallization in magnesium alloy, Mater Sci Forum 419–422: 509–514. https://doi.org/10.4028/www.scientific.net/MSF.419-422.509
[55] Yang X, Miura H, Sakai T (2004) Grain refinement in magnesium alloy AZ31 during hot deformation, Mater Sci Forum 467–470: 531–536. https://doi.org/10.4028/www.scientific.net/MSF.467-470.531
[56] Solas D E, Tome C N, Engler O, Wenk H R (2001) Deformation and recrystallization of hexagonal metals: modeling and experimental results for zinc, Acta Mater 49: 3791–3801. https://doi.org/10.1016/S1359-6454(01)00261-0
[57] Humphreys J F, Hatherly M (1995) Recrystallization and related Annealing Phenomena. Pergamon, Oxford, UK.
[58] Zhang Y, Wang J T, Cheng C, Liu J (2008) Stored energy and recrystallization temperature in high purity copper after equal channel angular pressing, J Mater Sci 43: 7326–7330. https://doi.org/10.1007/s10853-008-2903-8
[59] Dumitru F D, Ghiban B, Cabrera J M, Higuera-Cobos O F, Gurau G, Ghiban N (2014) Calorimetric analysis of a Mg-Zn-Zr alloy processed by equal channel angular pressing via route A, Key Eng Mater 583: 32–35. https://doi.org/10.4028/www.scientific.net/KEM.583.32
[60] Hajizadeh K, Alamdari S G, Eghbali B (2013) Stored energy and recrystallization kinetics of ultra-fine grained titanium processed by severe plastic deformation, Physica B 417: 33–38. https://doi.org/10.1016/j.physb.2013.02.031
[61] HadjLarbi F, Abib K, Khereddine Y, Alili B, Kawasaki M, Bradai D, Langdon T G (2013) DSC analysis of an ECAP-deformed Cu-Ni-Si alloy, Proceedings 22nd International Conference on Metallurgy and Materials. Brno, Czech Republic.
[62] Abib K, HadjLarbi F, Rabahi L, Alili B, Bradai D (2015) DSC analysis of commercial Cu–Cr–Zr alloy processed by equal channel angular pressing, Trans Non ferr Metals Soc China 25: 838−843. https://doi.org/10.1016/S1003-6326(15)63671-8
[63] Gao N, Starink M J, Langdon T G (2009) Using differential scanning calorimetry as an analytical tool for ultrafine grained metals processed by severe plastic deformation, Mater Sci Technol 25: 687–698. https://doi.org/10.1179/174328409X408901

[64] Dumitru F D, Higuera-Cobos O F, Cabrera J M (2014) ZK60 alloy processed by ECAP: Microstructural, physical and mechanical characterization, Mater Sci Eng A 594: 32–39. https://doi.org/10.1016/j.msea.2013.11.050
[65] Khereddine A Y, HadjLarbi F, Kawasaki M, Baudin T, Bradai D, Langdon T G (2013) An examination of microstructural evolution in a Cu–Ni–Si alloy processed by HPT and ECAP, Mater Sci Eng A 576: 149–155. https://doi.org/10.1016/j.msea.2013.04.004
[66] Doherty R D, Hughes D A, Humphreys F J, Jonas J J, Jensen D J, Kassner M E, King W E, McNelley T R, McQueen H J, Rollett A D (1997) Current issues in recrystallization: a review, Mater Sci Eng A 238: 219–274. https://doi.org/10.1016/S0921-5093(97)00424-3

Figures Caption

Fig. 1- DSC curves of Mg-1.43Nd processed by HPT after ½, 1, 5 and 10 turns, scanned at a heating rate of 20 °C/min.

Fig. 2- DSC scans of the recrystallization peak at a heating rate of 5, 10, 20 and 30 °C/min in Mg-1.43Nd alloy processed by HPT for up to 10 turns.

Fig. 3- Evolution of the temperature peak of recrystallization of Mg-1.43Nd as function of number of HPT turns.

Fig. 4- Boswell plots for Mg-1.43Nd deformed by HPT up to 10 turns for recrystallization peak.

Fig. 5- Evolution of activation energy of recrystallization of Mg-1.43Nd alloy as function of HPT turns.

Fig. 6- Recrystallized fraction for Mg-1.43Nd alloy after HPT processing up to ½, 1, 5 and 10 turns at 5 and 10 turns at different heating rates: a) 5, b) 10, c) 20 and c) 30 °C/min.

Table Caption

Table 1 Onset peak (T_0), offset peak (T_{max}), recrystallization temperatures (T_{rex}) and stored energy (E) obtained from the DSC curves at heating rate of 5 °C/min for Mg-1.43Nd alloy after HPT processing up to ½, 1, 5 and 10 turns.

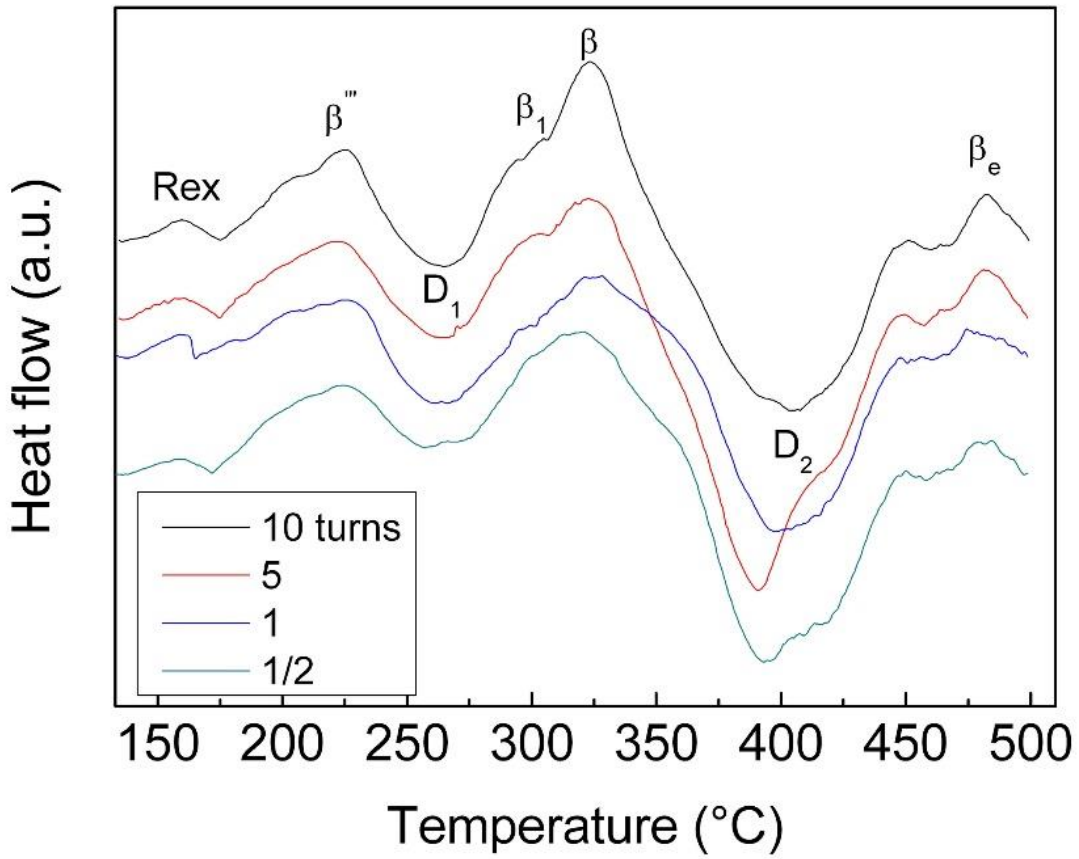

Fig. 1 DSC curves of Mg-1.43Nd processed by HPT after ½, 1, 5 and 10 turns, scanned at a heating rate of 20 °C/min.

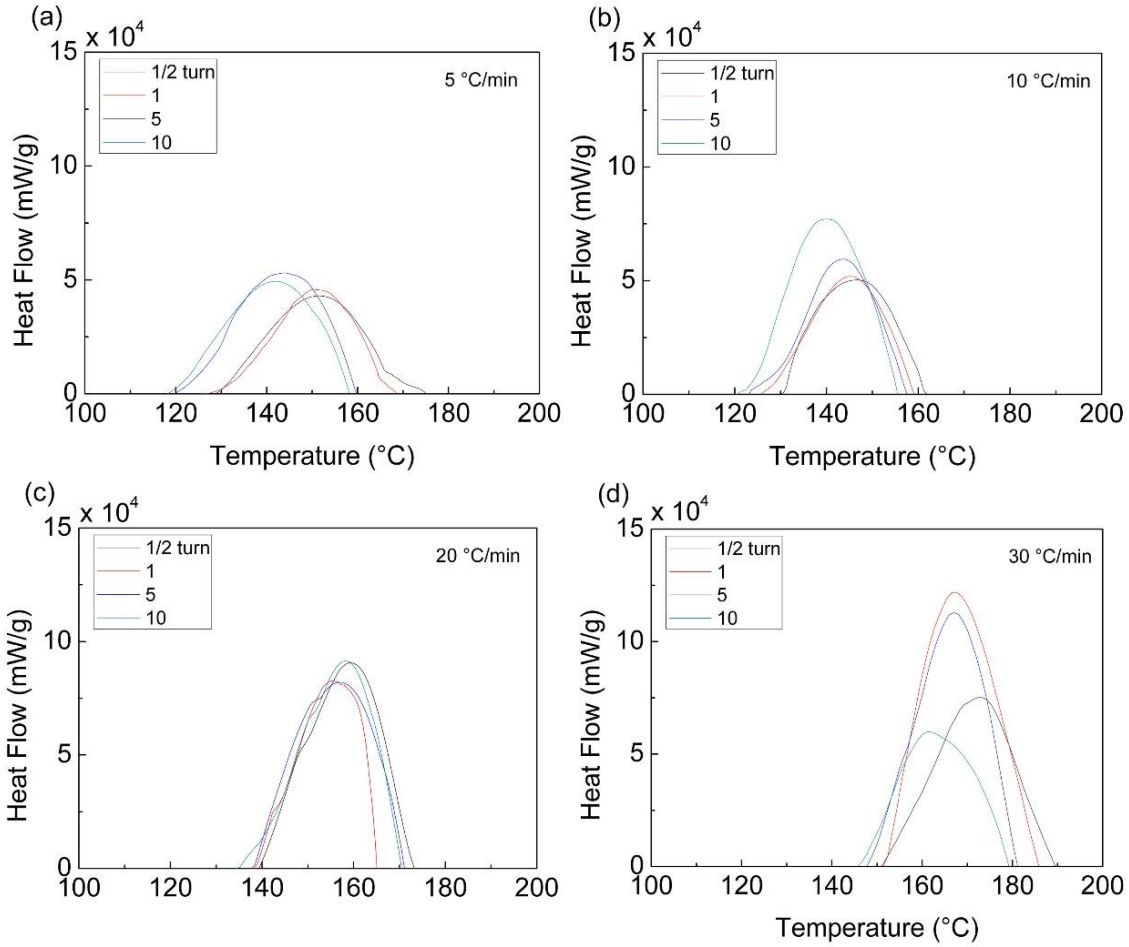

Fig. 2 DSC scans of the recrystallization peak at a heating rate of 5, 10, 20 and 30 °C/min in Mg-1.43Nd alloy processed by HPT for up to 10 turns.

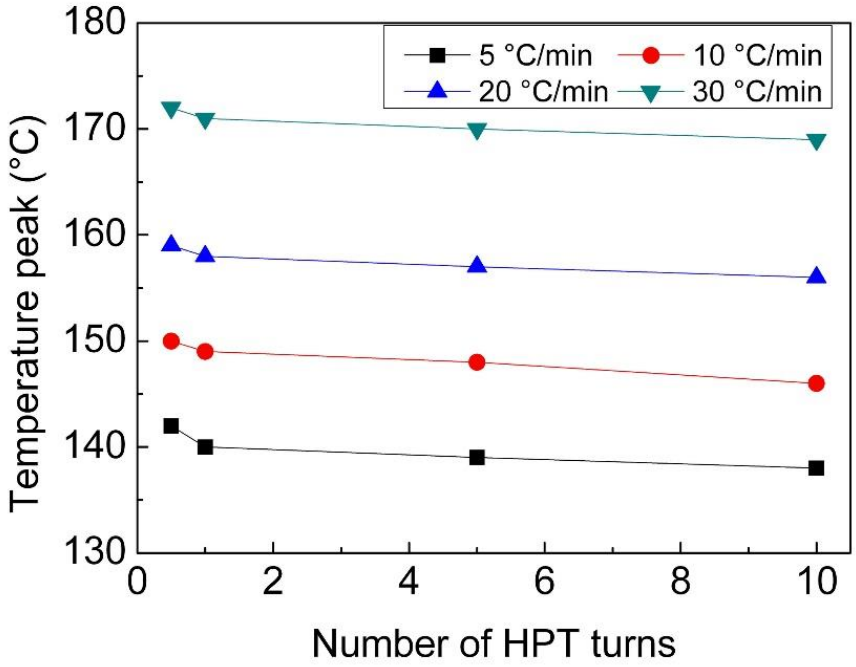

Fig. 3 Evolution of the temperature peak of recrystallization of Mg-1.43Nd as function of number of HPT turns.

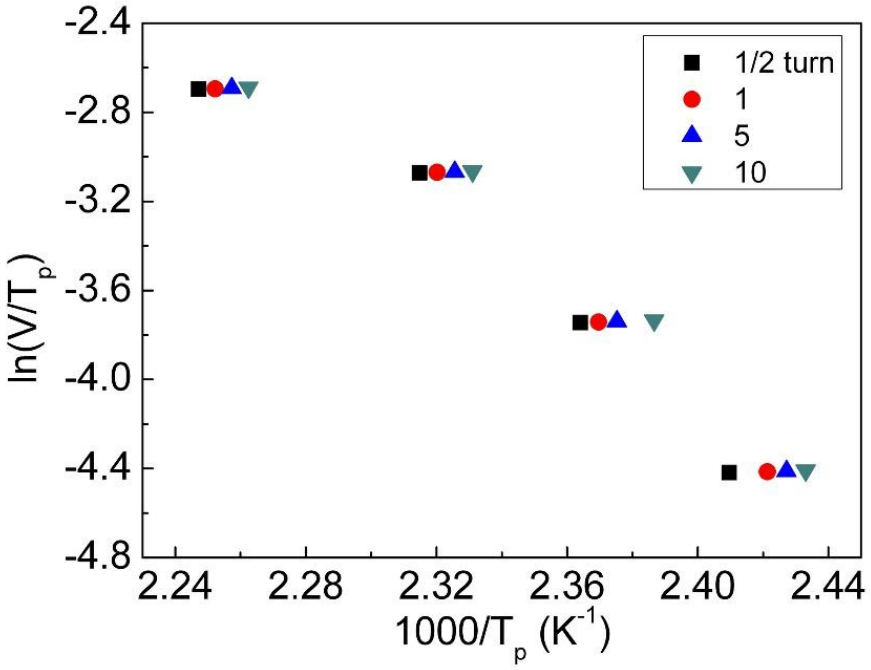

Fig. 4 Boswell plots for Mg-1.43Nd deformed by HPT up to 10 turns for recrystallization peak.

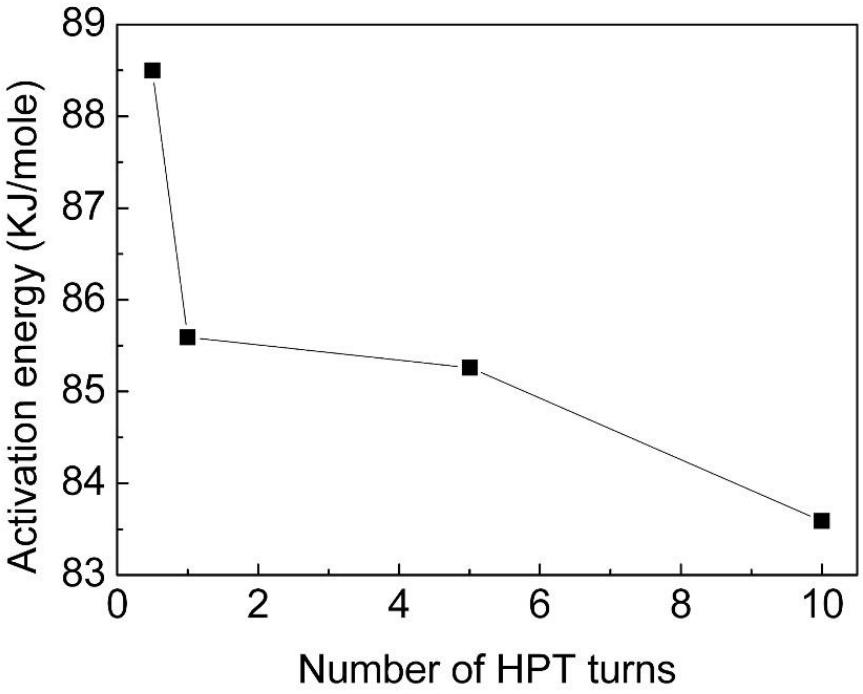

Fig. 5 Evolution of activation energy of recrystallization of Mg-1.43Nd alloy as function of HPT turns.

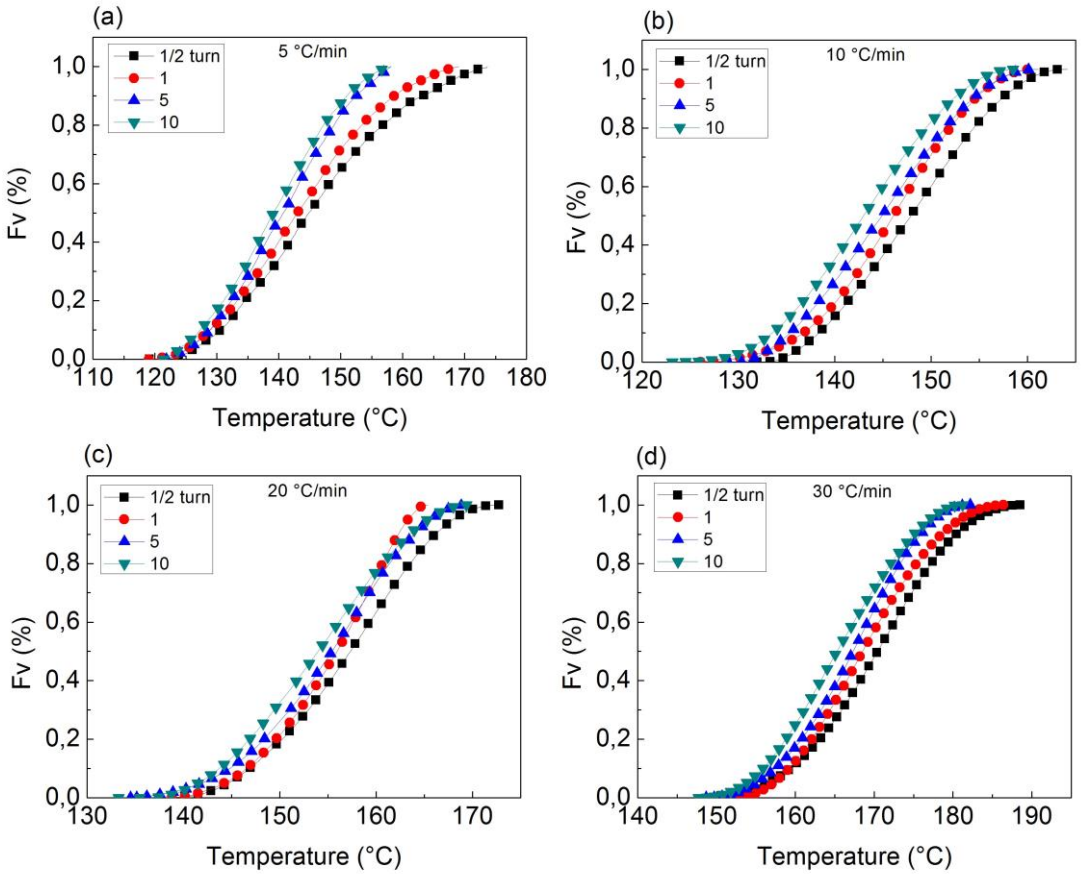

Fig. 6 Recrystallized fraction for Mg-1.43Nd alloy after HPT processing up to ½, 1, 5 and 10 turns at 5 and 10 turns at different heating rates: a) 5, b) 10, c) 20 and c) 30 °C/min.

Table 1 Onset peak (T_0), offset peak (T_{max}), recrystallization temperatures (T_{rex}) and stored energy (E) obtained from the DSC curves at heating rate of 5 °C/min for Mg-1.43Nd alloy after HPT processing up to ½, 1, 5 and 10 turns.

HPT turn	T_0 (°C)	T_{Max} (°C)	T_{Rex} (°C)	E (J/g)
1/2	114.2	166.1	144.6	1.64
1	119.0	169.0	142.8	1.95
5	121.3	158.0	140.6	1.72
10	121.8	158.1	138.9	1.33